JOURNAL OF AIRCRAFT
Vol. 48, No. 2, March–April 2011

Flyover Noise Measurements of a Spiraling Noise Abatement Approach Procedure

Lothar Bertsch*
DLR, German Aerospace Center, 38108 Braunschweig, Germany
Gertjan Looye†
DLR, German Aerospace Center, 82234 Wessling, Germany
Eckhard Anton‡
RWTH Aachen University, 52062 Aachen, Germany
and
Stefan Schwanke§
DFS Deutsche Flugsicherung GmbH, 63225 Langen, Germany

DOI: 10.2514/1.C001005

Alternative approach procedures are currently under investigation to evaluate their ground noise reduction potential. One such procedure involves approaching the airport at a considerably higher altitude compared with standard landing trajectories, followed by a spiraling descent (helix flight path) shortly before the runway threshold. In this way, high ground noise levels by approaching aircraft are dislocated away from the common approach path and concentrated in the area near the helix path, that is, in direct vicinity of the airport. Ground noise levels along the entire flight path before the helix are significantly reduced. The effectiveness of this procedure, referred to as "helical noise abatement procedure," has been quantified by means of computational simulation analyses. These analyses also focused on aspects such as increased fuel burn and the occurrence of multiple noise events below the helix. In June 2009, a new autopilot by the DLR, German Aerospace Center, especially capable of tracking curved flight-path trajectories, was flight tested. Three helical noise abatement procedures were included in the flight plan, as well as standard and steep landing approaches. In addition, dedicated flyover noise measurements were organized. Twelve ground microphones were placed along the common approach path and the helical flight segment. The measured data confirm the predicted noise dislocation effects. High noise levels were found to be limited to observer locations around the helix. Results from computational noise prediction have been compared with the experimental data. Predicted trends and noise dislocation effects are in good agreement with the measurements, whereas the absolute numerical values show discrepancies. The flight test was closely accompanied by a research and development member of the German air navigation service provider DFS Deutsche Flugsicherung GmbH to study the impact of spiraling procedures on air traffic management integration aspects and air traffic controller workload, for example, increased interaction with the pilots. Obviously, a spiraling approach procedure would not be implemented into the existing air traffic scenario with its common approach paths and more frequented airports. The operational and economic environment still need more detailed investigation. Helical approaches become more feasible for implementation at small, less-frequented regional airports or during night hours to avoid possible noise related curfews.

Nomenclature

D	=	diameter
h	=	altitude
mic x	=	ground microphone at location x
n_{turn}	=	number of full turns
R	=	Global Positioning System position
r	=	radius
SPL(A)	=	A-weighted sound pressure level, dBA
T	=	integration time for sound exposure level, s
t_{ref}	=	reference time for sound exposure level, s
V_{CAS}	=	calibrated airspeed
γ	=	inertial flight-path angle
σ	=	ground resistivity to air, $(\text{kN} \cdot \text{s})/\text{m}^4$
χ	=	inertial track angle

Subscripts

A	=	A-weighted level
center	=	helix center
end	=	end of flight segment
final	=	final straight segment
helix	=	helical flight segment
init	=	initial straight segment

Presented as Paper 2010-0011 at the 48th AIAA Aerospace Sciences Meeting, Orlando, FL, 4–7 January 2010; received 3 March 2010; revision received 6 December 2010; accepted for publication 7 December 2010.

*Institute of Aerodynamics and Flow Technology, Lilienthalplatz 7.
†Institute of Robotics and Mechatronics, Muenchner Strasse 20.
‡Institute of Aeronautics and Astronautics, Wuellnerstr 7.
§Am DFS-Campus 10.

I. Introduction

THE vast increase in commercial air traffic on the one hand and the growing pressure to reduce its environmental impact on the other hand require radical solutions to achieve considerably lower emission levels of noise and engine emissions. The solutions are sought both at the aircraft level, e.g., by development of more efficient and silent engines, as well as at the operational level, e.g., by developing more environmentally friendly takeoff and approach procedures.

To decrease aircraft noise levels in noise sensitive areas, a radical approach procedure is under investigation, the so-called helical noise abatement procedure [1] (HENAP). This procedure is based on concepts for simultaneous noninterfering operation by Hange and Eckenrod [2] and Young and Hall [3]. It involves the aircraft approaching the airport at a considerably higher altitude compared with standard instrument landing system (ILS) approaches and then performing a spiraling descent shortly before the runway threshold. The investigation was performed by means of computer analysis, using a new tool set by the DLR, German Aerospace Center (hereinafter referred to as DLR), for the environmental analysis of aircraft flight trajectories. The process comprises tools for aerodynamics, flight mechanics, engine cycle modeling, and the prediction of aircraft noise and engine emission [1].

The main conclusions from this computational study are the following: depending on the initial approach altitude and the geometry of the helix (number of full turns, turn radius, rate of descent, etc.), the high ground noise levels of approaching aircraft are dislocated away from the common ILS approach path into the area around the spiraling descend. This will significantly reduce ground noise impact along the entire flight path before the helix. Yet, at the same time, each approaching aircraft causes multiple flyover events in the vicinity of the helix, hence increasing ground noise pollution in this area. Furthermore, fuel use and flight time increase along the helical approach procedure compared with ideal and short direct ILS approaches.

In parallel to the computer analysis a flight test was prepared to evaluate a newly developed autopilot with improved weather capabilities [4]. To this end, the autopilot was implemented on DLR's advanced technologies testing aircraft system (ATTAS, see Fig. 1). The intention was to test this autopilot in the form of a helical inertial flight trajectory at a constant airspeed, since this causes lateral and horizontal wind shears, even in the presence of a little steady wind. The idea arose to perform this test trajectory in the form of a landing approach, resulting in the aforementioned HENAP trajectory. After it turned out that this was possible from an operational and safety point of view, it was decided to combine the flight test with a ground noise measurement campaign. This would allow for validation of the HENAP results from the computational analysis, in particular to confirm the predicted noise reduction potential. The HENAP obviously raises operational question marks, such as air traffic control aspects, which had not been considered so far. For this reason, a representative of the German air navigation service provider DFS Deutsche Flugsicherung GmbH observed the approaches from the airport tower.

This paper describes the flight test and presents the results. It is structured as follows: in Sec. II the HENAP will be described in more detail. In Sec. III the computational noise analysis of the HENAP and some illustrative results will be presented; Sec. IV describes equipment, preparation, and actual execution of the flight test; Sec. V discusses initial results, including the validation of basic principles of the HENAP, the computational noise analysis and the performance of the autopilot, as well as operational aspects based on crew comments and observations from the airport tower; finally, conclusions will be discussed in Sec. VI.

II. Spiraling Approach Procedure

The HENAP trajectory and its main characteristic parameters are depicted in Fig. 2. The trajectory consists of three segments. The first, initial segment is a straight path, which is easily captured by the lateral/vertical navigation autopilot modes and allows the aircraft to be configured for the second, helical segment. Geometrically, the actual helix is initiated at the point where the initial straight segment perpendicularly passes the helix center. Practically, the procedure is initiated slightly earlier in order to allow the aircraft to smoothly roll into the turn. After the helical segment, the trajectory ends with straight approach segment, allowing the aircraft to be brought in trimmed, wings-level flight, from where the autopilot may switch to its landing modes (flare, retard, decrab) or from where the pilot may take over. The final segment will be identical to the standard runway approach path; its length will be a compromise between safety and its effectiveness for noise abatement (the shorter the better).

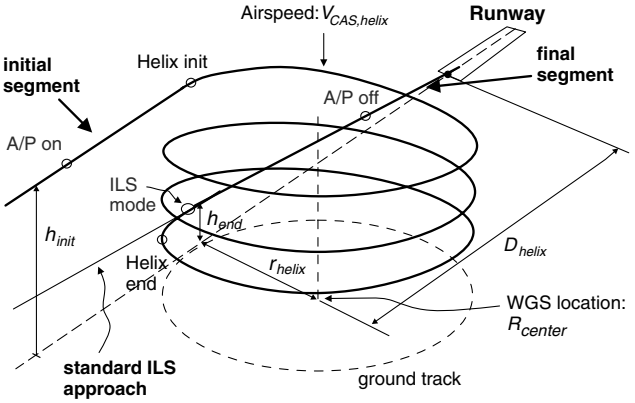

Fig. 2 HENAP: parametric definition.

The parameters R_{center}, r_{helix}, $V_{\text{CAS,helix}}$, and h_{end} may be (slowly) changed during the maneuver. The entry height h_{init}, the final altitude h_{end}, and the number of turns determine the rate of descent (altitudes are barometric, question nil height). The flight-path and track angles of the final segment are determined by the runway heading and glide slope angle. In Fig. 2 the flight-path angle of the initial segment (γ_{init}) is zero. This is not a prerequisite, as will be shown in the simulation studies. The same holds for the initial track angle χ_{init}. In the figure it is identical to the runway heading, but the spiraling descent may start from any direction.

III. Computational Analysis of the HENAP

A new tool set for the environmental analysis of aircraft flight trajectories has been applied to investigate spiraling approach procedures [1]. Noise shielding effects and the overall ground noise impact are predicted with the new DLR tools SHADOW [5] and "parametric aircraft noise analysis module" (PANAM) [6], respectively. Predicted noise isocontour plots illustrate the concept of spiraling noise abatement approach procedures at standard atmosphere condition with no wind for a conventional transport aircraft with under-the-wing engine installation. The maximum SPL_A noise footprint for this aircraft along the reference approach is depicted in Fig. 3a. Isocontour areas for the investigated helical approaches with 2, 3, and 4 helical flight segments are shown in Figs. 3b–3d respectively. Maximum SPL_A levels along each flight ground track are depicted in Fig. 4. Flight-path angles were held constant and limited to $-3°$. A constant helix radius r_{helix} of 2000 m was selected for the coordinated turns to guarantee passenger comfort by preventing high bank angles and decelerations. According to the selected parameters, load factor n and bank angle β during the spiraling segments were limited to 1.15 and 30°, respectively. To maximize ground noise reduction along the HENAP, the initial flight segment before the helix was simulated identical to the reference approach with a glide slope γ_{init} of $-3°$.

A considerable increase in flight time, fuel consumption, and gaseous emissions is predicted for all helical approaches if compared with the reference approach, as presented in Table 1. It has to be noted that the selected reference procedure is a direct, straight-in approach, i.e., the path is aligned with the runway heading. Obviously, an

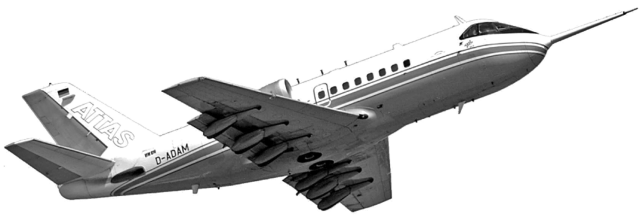

Fig. 1 Flying test bed ATTAS of the German Aerospace Center.

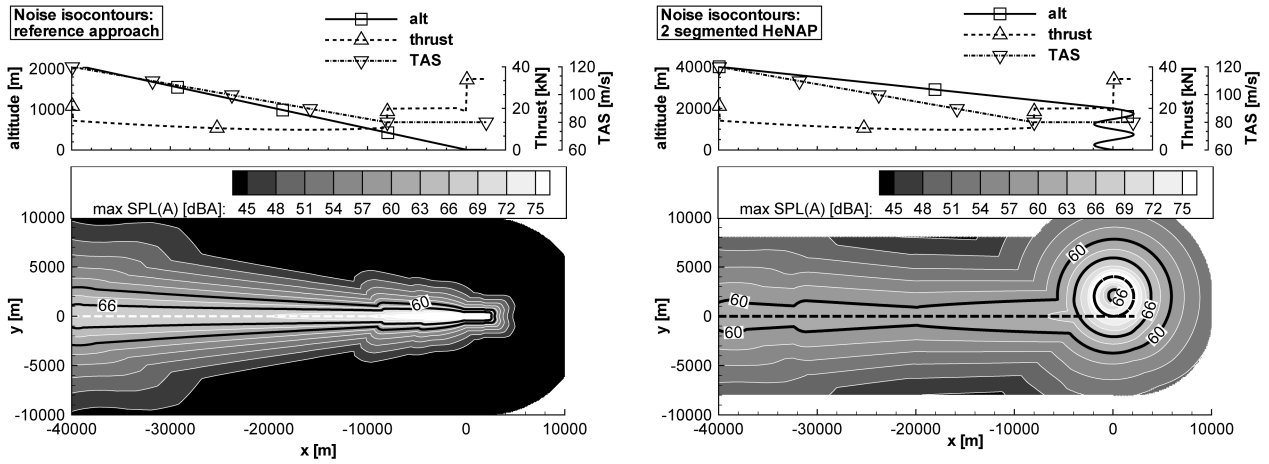

a) Reference approach

b) HeNAP: 2 helical segments

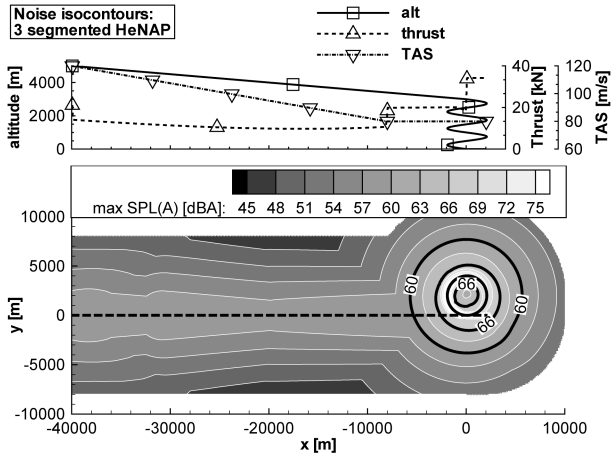

c) HeNAP: 3 helical segments

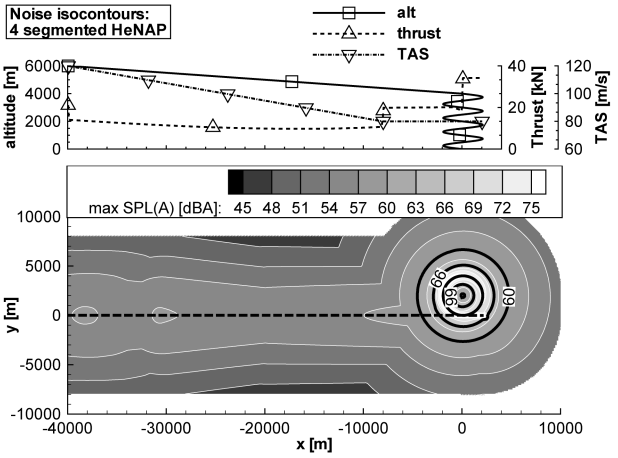

d) HeNAP: 4 helical segments

Fig. 3 Predicted maximum SPL_A isocontour plots for conventional, medium-range transport aircraft.

arrival from any other direction would require more rerouting hence lead to an extended flight path. A case-specific tradeoff, i.e., consideration of routing in the proximity of the airport and possible direct shortcut by spiraling descent operation (see Fig. 5a), between economical flight performance and low-noise operation becomes inevitable.

Comparing the reference noise isocontour areas with the HENAP isocontour lines demonstrates the significant noise reduction potential before the spiraling flight segments. The highlighted lines in each plot represent selected isocontour areas. High noise levels are dislocated away from the common approach path and concentrated within an area around the ground track of the helical flight segment. Obviously, this limited area will then be subject to multiple flyover events for each approaching aircraft hence increased noise pollution. The isocontour plots show the maximum noise levels that have been predicted for each flyover event.

Ideally, the helix location can be selected in such a way that high noise levels are kept within airport borders or limited to low-populated regions and industrial zones. To further illustrate this, an airport with optimal geographical location was identified without consideration of air traffic management aspects. A three-segmented HENAP and a conventional approach, FUTSU night north arrival, on runway 34 L of Tokyo Haneda International Airport [International Civil Aviation Organization (ICAO) airport code RJTT], have been simulated. The simulation of the FUTSU approach is based on official approach charts by the Civil Aviation Bureau of Japan [7]. The procedure is designated for night operation in order to reduce community noise annoyance mainly for the Boso Peninsula. The resulting significant detour around the peninsula is depicted in Fig. 5a.

A new shortcut from waypoint HONDA directly toward the airport, waypoint FAF, followed by a spiraling flight segment was established. The new flight route has been simply copied onto a map to demonstrate the concept (see Fig. 5b). Following the new shortcut, aircraft can remain on flight level 80 until reaching the spiraling flight segment. Hereby, ground noise impact is dislocated away from populated areas and concentrated over the Tokyo Bay (see Figs. 5c and 5d). Initial simulation results indicate a reduction of the flight path by more than 50% along with significant environmental benefits due to the HENAP.

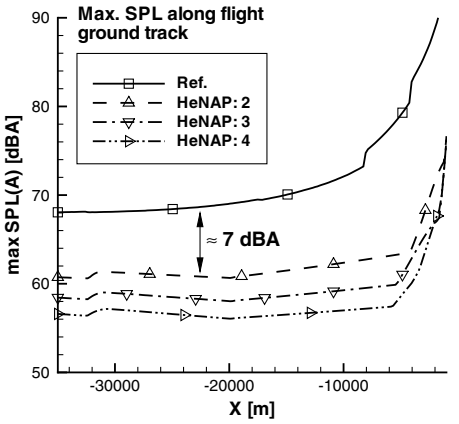

Fig. 4 Predicted maximum SPL_A along flight ground tracks for conventional, medium-range transport aircraft.

Table 1 Predicted environmental effects: HENAP vs reference approach

Procedure	60 dBA isocontour area, km^2	65 dBA isocontour area, km^2	70 dBA isocontour area, km^2	Fuel, kg	NOx, kg	Flight time, s
Reference approach	78.05	41.66	7.01	208.56	1.71	450.5
HENAP 2	199.67	55.01	26.08	299.05	2.34	675.5
HENAP 3	102.63	39.03	12.77	329.08	2.37	833.0
HENAP 4	67.73	29.74	14.60	363.21	2.50	971.5

IV. Flight-Test and Flyover-Noise Measurements

A. Test Aircraft and Autopilot

The flight test was carried out to develop methods for the design of feedback flight control laws to considerably improve aircraft closed-loop behavior under adverse atmospheric conditions. The autopilot control laws flown during the described test flight are described in more detail in [4]. Although it contains most modes of operation of standard autopilots (including autoland), for the test flight its modes for helix tracking and steep landing approaches were of particular interest.

Tracking a helical flight path is a challenging task for an autopilot and very suitable for assessing its overall behavior and capabilities. During a helix maneuver, one basically encounters a considerable amount of challenges in autopilot design: coordination of longitudinal and lateral modes, accurate tracking of a flight path that is continuously "bending away," and combined tracking of inertial (the flight path) and air-mass-based references (the airspeed). From an atmospheric point of view, during a helix maneuver even little constant wind results in continuous wind shears in lateral and longitudinal directions.

For the flight test, the autopilot control laws were implemented on DLRs ATTAS (see Fig. 1). The aircraft is based on a VFW 614 civil transport aircraft equipped with two Rolls–Royce M45 H engines. ATTAS is equipped with a unique in-flight simulation architecture and a fly-by-wire flight control system, allowing for implementation of new flight control laws with low effort. Before flight, the complete flight plan was reviewed and tested in the ATTAS ground-based flight simulator. Since the flight control laws were tested in flight for the first time, the initial segment was chosen to be straight and level, i.e., $\gamma_{\text{init}} = 0$. Three turns were selected, which is a compromise between time for control law evaluation and available flight time.

B. Flight-Test Plan

The flight-test plan consisted of seven approaches to runway 26 of the Forschungsflughafen Braunschweig (ICAO airport code EDVE). The aircraft's configuration along all flights was held constant, in order to reduce complexity of the procedures and ensure a sufficient offset between ambient and flyover noise levels, with gear deployed and flaps at 14°. The reference time (flight time) for overall data correlation was initialized, i.e., flight time set to 0.0 s, along each test

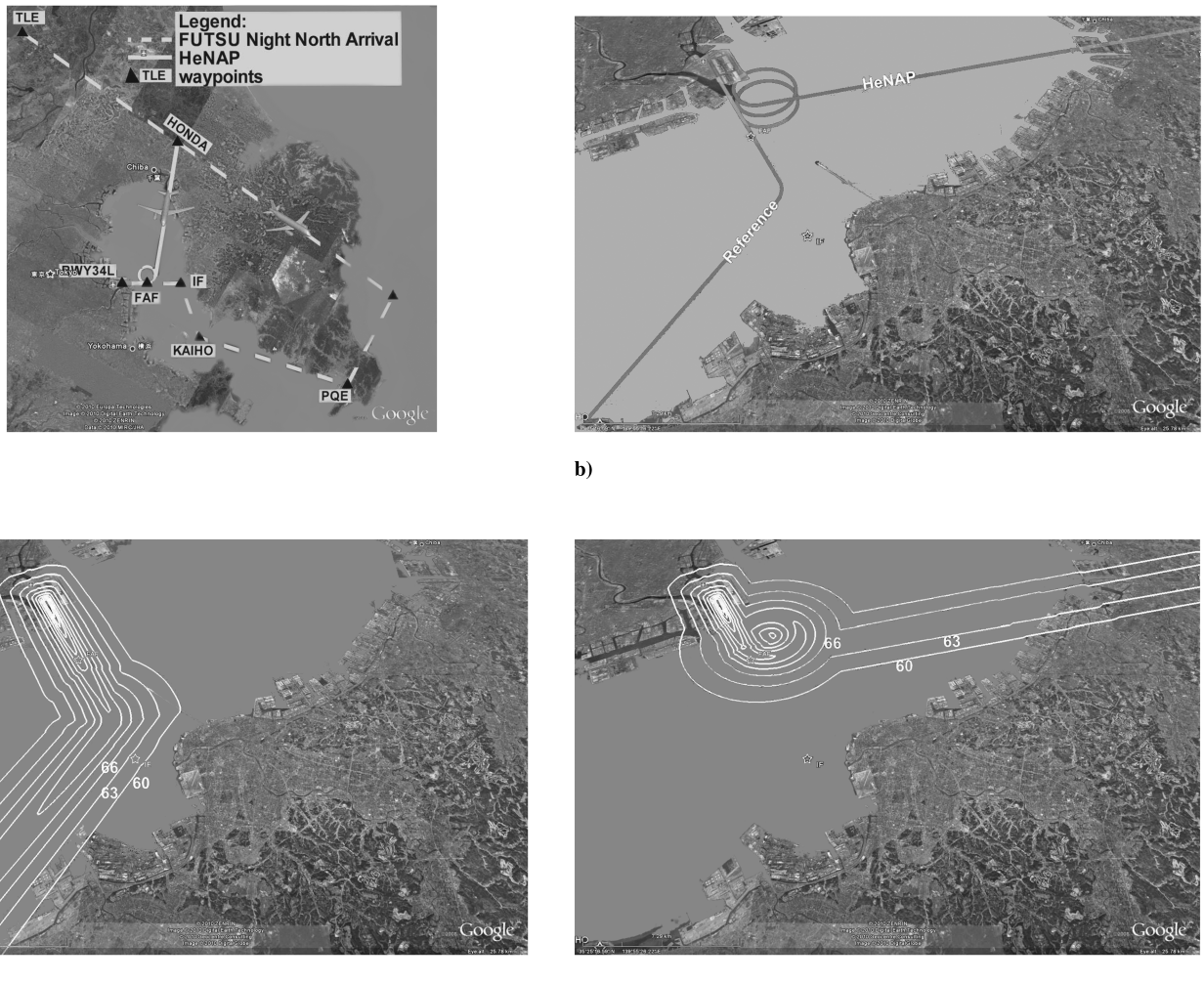

Fig. 5 Tokyo Haneda International Airport, night operation scenario: HENAP vs FUTSU night north arrival [7] (Google Earth).

flight at a ground distance of 12 km to the runway threshold. The first test flight is a standard 3° ILS approach followed by a go-around when reaching 500 ft above ground level (AGL). The second and third test flights are steep approaches with glide slopes of 6–7° starting at a barometric altitude of 3000 ft question nil height (QNH). The common ILS path is captured from above, and go-around is initiated when reaching 500 ft AGL. The objectives were to test the vertical path and speed modes, and vertical path and glide slope capture logic. Flights four to six are HENAP starting at an altitude of 7500 ft. ILS path is captured after the last turn, followed by a go-around when reaching 500 ft AGL. The flight-path angle γ_{init} along the initial flight segment was set to zero for simplicity. This maneuver was intended as the all-up test of the autopilot control laws. Finally, flight seven is the second standard ILS approach, continued into the landing and rollout (performed manually), marking the end of the test flight.

C. Procedures

The helical approach trajectory is depicted schematically in Fig. 2. As already mentioned before, the maneuver is initiated in an altitude h_{init} of 7500 ft QNH in the direction of the runway. The altitude is held constant ($\gamma_{\text{init}} = 0$) until the aircraft passes the helix center, which is located to the right. The helix center in turn is located at a distance D_{helix} of 3200 m before the runway threshold. The latter point is also the reference for computing local x, y, z coordinates. After exactly three full turns with a radius r_{helix} of 2000 m the maneuver ends with the final straight trajectory, which matches the standard ILS approach path. Shortly before ending the final circle, the ILS signal is checked. If the aircraft is within the cone, the autopilot changes into its ILS tracking mode. Otherwise, flight continues in runway direction, but at constant altitude. The airspeed $V_{\text{CAS,helix}}$ is held constant at 160 kt (82 m/s). During the final quarter of the last turn, it is reduced to the agreed final approach speed $V_{\text{CAS,helix}}$ of 140 kt (72 m/s).

The steep approaches were initiated at an altitude of 3000 ft QNH. The transition from steep into the standard approach path was planned at the same distance D_{helix} from the runway threshold as the helix center. The transition from horizontal into the steep approach was fixed to an altitude of 6500 ft. In this way, the trajectory is fully defined. An approach speed of 140 kt (72 m/s) calibrated airspeed was selected. The procedure is flown automatically by the new autopilot and switch-on and switch-off positions are labeled as *A/P on* and *A/P off* (for autopilot on and off, respectively) in Figs. 2 and 6.

D. Test Setup

1. Noise Measurement Equipment and Data Acquisition System

The flight trajectories and corresponding operational aircraft data were recorded on board of the ATTAS aircraft. The trajectory data contained GPS time for synchronization with measured ground noise data. In addition to official airport weather data, ambient temperature, relative humidity, static air pressure, and wind speed/direction have been obtained every 15 min during the flyover campaign using a pole mounted weather sensor system installed close to location mic 8. The data was measured 10 m above the ground, according to the aircraft noise certification standards [8].

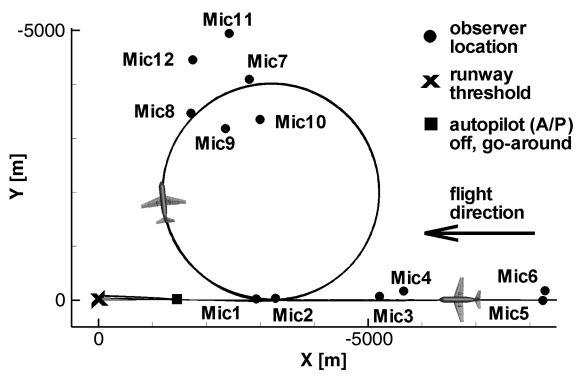

Fig. 6 Observer locations along flight ground tracks.

Table 2 Location coordinates

Location	x, m	y, m	World geodetic system[a] coordinates
Mic 1	−2924.32	−21.55	N 52.3222, E 10.6067
Mic 2	−3281.34	−34.93	N 52.3226, E 10.6119
Mic 3	−5210.96	−64.57	N 52.3245, E 10.6400
Mic 4	−5661.15	−164.67	N 52.3257, E 10.6465
Mic 5	−8239.39	6.07	N 52.3263, E 10.6844
Mic 6	−8283.45	−172.10	N 52.3279, E 10.6848
Mic 7	−2796.36	−4092.50	N 52.3586, E 10.5994
Mic 8	−1713.22	−3463.96	N 52.3520, E 10.5844
Mic 9	−2355.22	−3176.19	N 52.3500, E 10.5942
Mic 10	−2995.14	−3348.14	N 52.3521, E 10.6033
Mic 11	−2425.86	−4943.79	N 52.3659, E 10.5929
Mic 12	−1750.79	−4456.68	N 52.3610, E 10.5836
Helix center	−3200.0	−2000.0	N 52.3399, E 10.6079
RWY 26	0.0	0.0	N 52.3196, E 10.5640

[a]WGS84.

Noise data were acquired using an autonomous field noise measurement system consisting of plate mounted microphones and a laptop-based data acquisition system conforming to DIN EN 61265. The digitized sound pressure signal was recorded with a sampling rate of 48 kHz and a 16 bit resolution. The measurement system further included a GPS unit which allows the GPS time and the pulse-per-second to be recorded along with the sound pressure signal for data synchronization. Furthermore, the GPS position is stored in the noise data header which allows for the precise determination of the geometric relation between aircraft trajectory and microphone position on the ground. A ground board microphone arrangement was chosen originally developed for noise certification of General Aviation aircraft (ICAO Annex 16, Chapter 10). Each microphone is mounted eccentrically in an inverted position at 7 mm above the circular metal ground plate. This setup is used to minimize interference effects in the frequency range from 50 Hz up to 10 kHz typically used for aircraft noise analysis. Detailed analysis of the interference characteristics of this microphone setup can be found in [9,10]. Signal processing and calculation of the SPL_A was performed according to the aircraft noise certification standards [8].

No noise data correction, e.g., de-Dopplerization and correction for atmospheric absorption, was applied because the focus of the campaign was on the one hand to evaluate ground noise impact instead of noise emission at the source and on the other hand to provide uncorrected noise data to validate the prediction codes.

2. Observer Locations

A total of 12 microphone stations were installed around Forschungsflughafen Braunschweig. Observer locations along the flight ground track of the common approach path and of the HENAP have been selected. Six microphones have been installed along the common approach path and the helical flight segments, respectively. The coordinates for the ground microphones are given in Table 2 and the layout is depicted in Fig. 6. All flights are approaching from the east toward EDVE runway 26. The locations mic 1 to mic 6 along the common approach path have been selected such that the noise reduction potential of the steep approach and the HENAP compared with the reference path can be demonstrated. Locations along the helical flight ground track have been selected in order to investigate noise emission along the curved flight segments, locations mic 7 to mic 12.

V. Analysis of Flight-Test Results

A. Tracking of the Flight Path

Figure 6 depicts one HENAP, one steep, and one standard approach trajectory out of the seven approaches performed during the flight test. The three HENAP approaches turned out to be nearly identical. As a result, the projection all HENAP trajectories on the

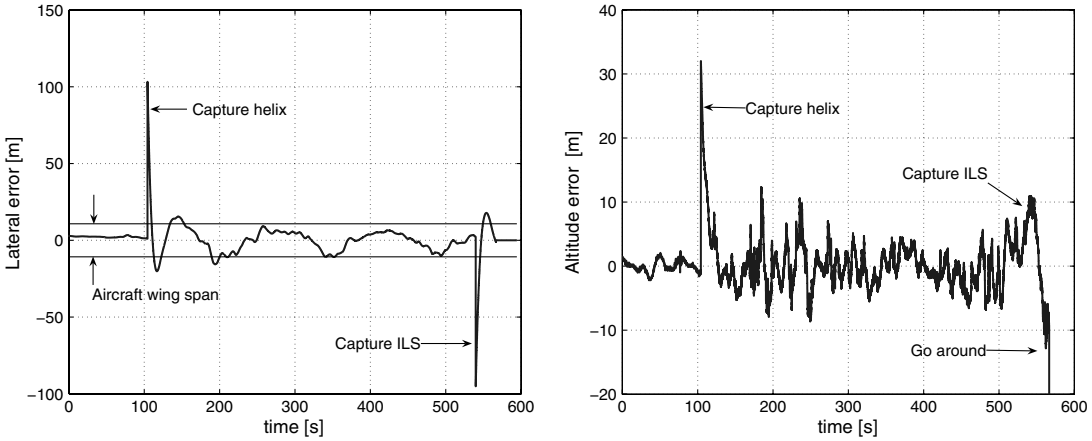

a) Lateral path deviation during first helix approach **b) Altitude error**

Fig. 7 Flight data visualization.

ground are nearly perfect circles and hardly distinguishable. From an autopilot design point of view, this of course is very encouraging since the winds were quite significant. Regarding the steep approaches, the second one was slightly steeper due to the somewhat higher initial altitude. The path tracking accuracy is confirmed by Fig. 7a (lateral path error during first helical approach) and Fig. 7b (altitude error during first helical approach). The time along the helix path has been stretched along the x axis while the deviations are represented on the y axis. The larger peaks at the beginning and the end are caused by switching to and from the spiral mode. Their quick reduction illustrates the good tracking capability of the autopilot. More details on the behavior of the autopilot can be found in [4].

The recorded thrust, speed, and altitude profiles for each test flight are depicted in Fig. 8. Obviously, the operating conditions along identical flight procedures are in close proximity hence the corresponding noise emission should be quite similar as well (note: constant aircraft configuration).

The behavior of the autopilot regarding piloting technique, e.g., throttle activity, was received well by the pilots. During the maneuver, ride quality (load factors, intercepts, etc.) was of no concern.

B. Measured Noise Levels

The wind conditions on the only available test day were adverse for flyover noise measurements. Wind gusts up to 15 kt have been

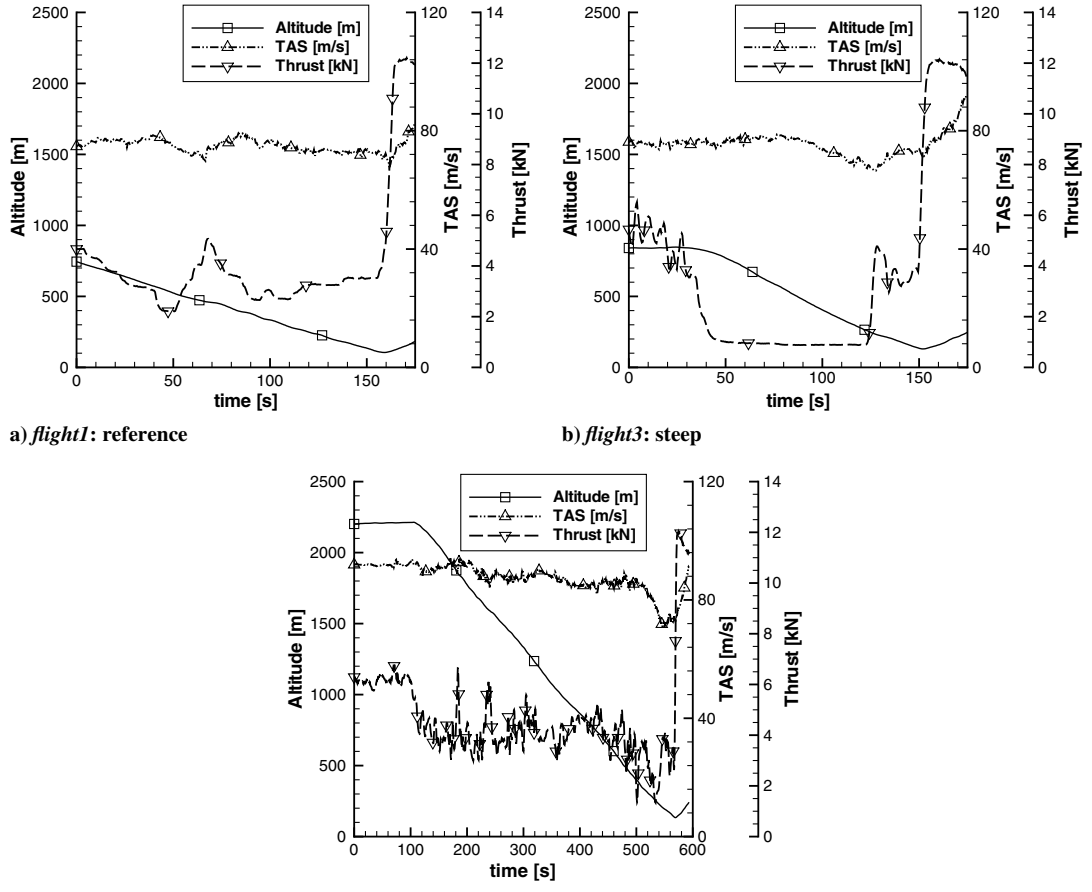

a) *flight1*: reference **b) *flight3*: steep**

c) *flight4*: HeNAP

Fig. 8 Flights 1 (reference), 3 (steep), and 4 (HENAP): recorded thrust, true airspeed, and altitude history (constant configuration: gear deployed, flaps at 15°).

recorded on the ground. At the airport winds between 15 and 20 kt with direction ≈255° (runway heading 265°) were measured. At higher altitudes winds up to 28 kt were encountered. Between and below clouds (broken cumulus, base ≈4000 ft, top ≈7000 ft) thermal turbulence was encountered. In the clouds, turbulence levels were considerably higher.

ICAO weather conditions for noise certification according to Annex 16, Appendix 2,2.2.2 [8] are the following: temperatures between 2 and 35°C; no rain, dew, or snow; no ground-based temperature inversions; humidity between 20 and 95%; wind conditions 10 m above ground, average wind $\leq$ 12 kt, average crosswind $\leq$ 7 kt, maximum wind $\leq$ 15 kt, maximum crosswind $\leq$ 10 kt). Therefore, the measured noise levels should be examined critically and should not directly be compared with data from other campaigns under certified wind conditions. The weather and wind conditions did not change significantly during the 2 h of the test flights hence the influence of wind on the measured data is assumed to be similar for all recorded flight events. This approximation is confirmed by only small variations in the measurements for identical approach procedures, i.e., agreement between level time histories for flights 4 to 6 (HENAP), flights 1 and 7 (reference), and flights 2 and 3 (steep), respectively. Recorded time-level histories of the *A*-weighted sound pressure level (dBA) are depicted in Figs. 9 and 10. The depicted flight time was initiated for each test flight at a ground distance of 12 km to the runway threshold. Despite the adverse weather conditions, the recorded sound pressure level time histories reveal very low background noise levels for all microphone locations of 55 dBA down to 50 dBA at some locations. The maximum sound pressure levels of the aircraft flyover events are therefore more then 20 dB above the ambient noise levels, which is the required margin for noise certification measurements. This supports the suitability of the measured noise data for comparing the noise impact among the tested approach procedures. At locations mic 1 to mic 6 the noise levels for all seven test flights have been recorded. At the remaining locations only the HENAP noise was perceived.

Noise levels at locations mic 5 and mic 6 are compared, to evaluate the potential noise reduction of the tested procedures along the common approach path. Noise level differences with respect to data of flight 1, presented in Table 3, indicate the anticipated noise relocation effects at locations mic 5 and mic 6 due to the spiraling and steep approaches.

All test flights pass the ILS_{mode} marker, depicted in Fig. 2, with identical altitude, speed, and thrust setting. Therefore, microphone locations in close proximity to this marker are exposed to similar noise peaks along each flyover event. Figure 11 shows the measured noise levels along the spiraling segments of flight 4. The aircraft following the HENAP is consecutively flying over mic 1, mic 8, and mic 7. Each of these individual flyover events can be identified and correlated (see Fig. 11a). The measured noise levels inside and outside of the helix do not significantly deviate from each other. Figures 11b and 11c show similar noise impact inside and outside off the helix along flight 4. Overall, the maximum noise levels measured below the helical flight segments are comparable to noise levels recorded below the standard ILS approach path. Comparing the recorded noise levels for the reference approach with measurements of the HENAP does not indicate additional ground noise increase due to the curved flight segments, e.g., comparing levels at location mic 1 (Fig. 9a) with levels recorded at location mic 8 (Fig. 10a).

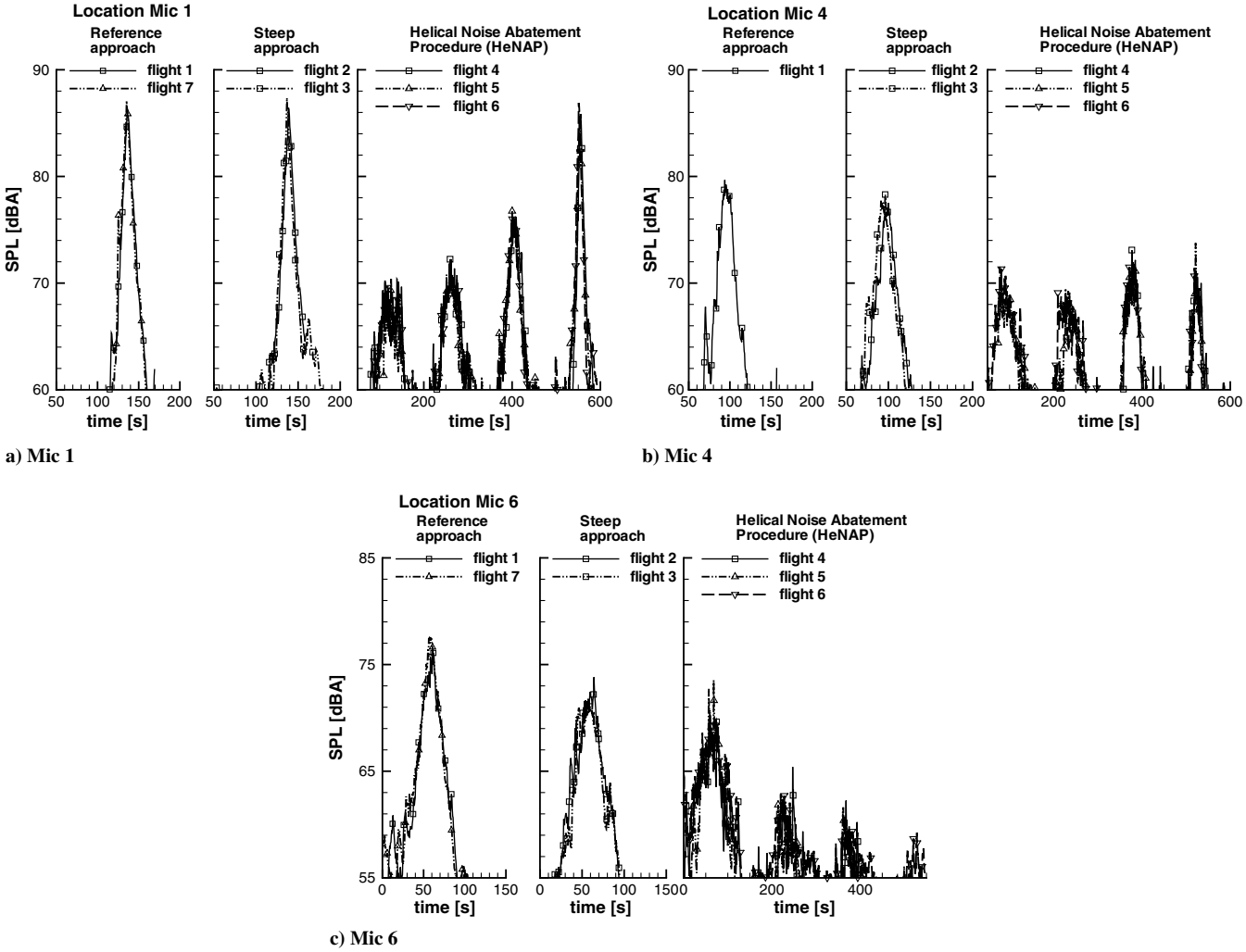

Fig. 9 Measured SPL_A time history at the locations mic 1, mic 4, and mic 6.

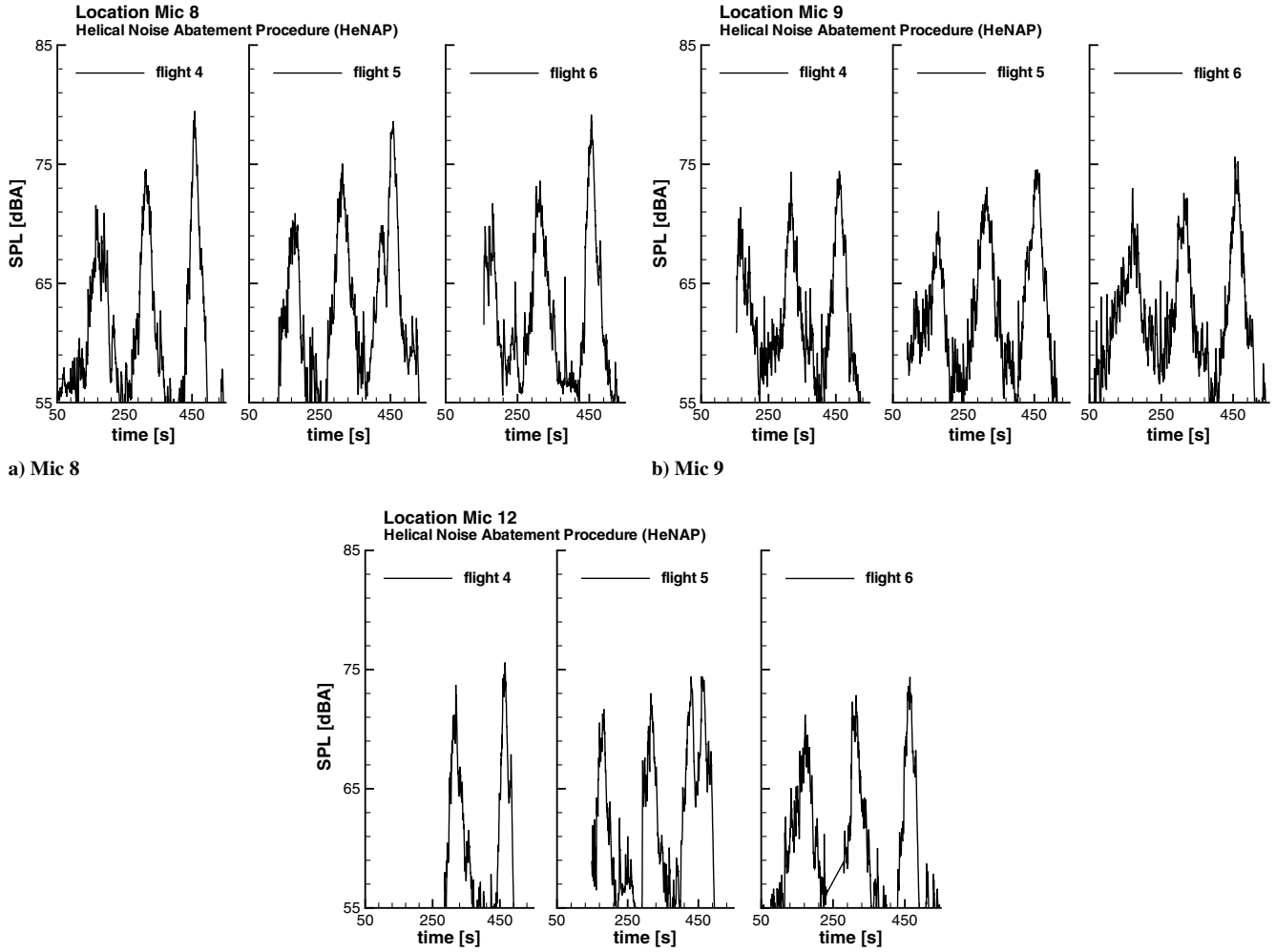

Fig. 10 Measured SPL_A time history at the locations mic 8, mic 9, and mic 12.

To study the impact of multiple flyover events on community noise annoyance the sound exposure level (SEL) is a common indicator. Therefore, recorded SPL_A time histories along the common approach path as well as along the spiral are translated into SEL levels according to Eq. (1):

$$\mathrm{SEL} = 10 \cdot \log 10\left(\frac{1}{t_{\mathrm{ref}}}\int_0^T 10^{\mathrm{SPL}_A(t)/10}\,\mathrm{d}t\right) \tag{1}$$

with $t_{\mathrm{ref}} = 1$ s and the integration time T equals the measurement time.

The SEL is mainly dominated by the maxima of recorded sound pressure levels but also influenced by multiple flyover events. The levels according to the measurements are presented in Table 4.

Each HENAP causes multiple flyover events resulting in several noise peaks of varying levels as depicted in Figs. 9 and 10. At the locations along the spiral, only HENAP noise was experienced, hence, no flyover but ambient noise is prevalent during the reference and steep approaches. Obviously, the area along the spiral is only exposed to aircraft noise during HENAP operation, i.e., these areas are suddenly exposed to SEL levels over 80 dBA. The levels directly under the spiral, e.g., mic 8, are exposed to SEL levels comparable to measurements directly under the reference approach path.

Corresponding to the SEL_A time histories at mic 1, steep, reference and HENAP approach show similar SEL levels. With increasing distance to the helix center, the situation becomes more advantageous for the HENAP. Starting along the common approach path at a distance of less than one spiral diameter from the helix center, the SEL levels of steep and HENAP approach are lower than the corresponding levels of the reference approach. Obviously, multiple flyover events are compensated by significantly reduced SPL_A levels. This advantage for the HENAP will increase along the common approach path with distance to the helix center.

C. Measured vs Predicted Noise Data

Strong winds and wind gusts are known to distort the sound field in an uncontrolled manner hence complex noise shielding effects are corrupted. Therefore, the current data was not considered appropriate to validate the new DLR noise shielding code SHADOW [5] hence the noise shielding effects were neglected in the comparison.

Recorded flight-test data are provided as input for the computational noise prediction, whereas the prediction in Sec. III is based on simulated input data. Noise prediction with PANAM [6] is based on semi-empirical, parametric noise source models to quickly identify low-noise aircraft designs and noise abating flight trajectories. Major aircraft noise sources are modeled but interactions

Table 3 Recorded maximum SPL_A differences ΔdBA with respect to flight 1 (reference) at locations mic 5 and mic 6

Flight	Type	Mic 5	Mic 6
Flight 2	Steep	−4.0	−5.0
Flight 3	Steep	−4.5	−6.0
Flight 4	HENAP	−7.5	−8.5
Flight 5	HENAP	−7.5	−7.0
Flight 6	HENAP	−6.5	−9.0
Flight 7	Reference	+1.5	+1.0

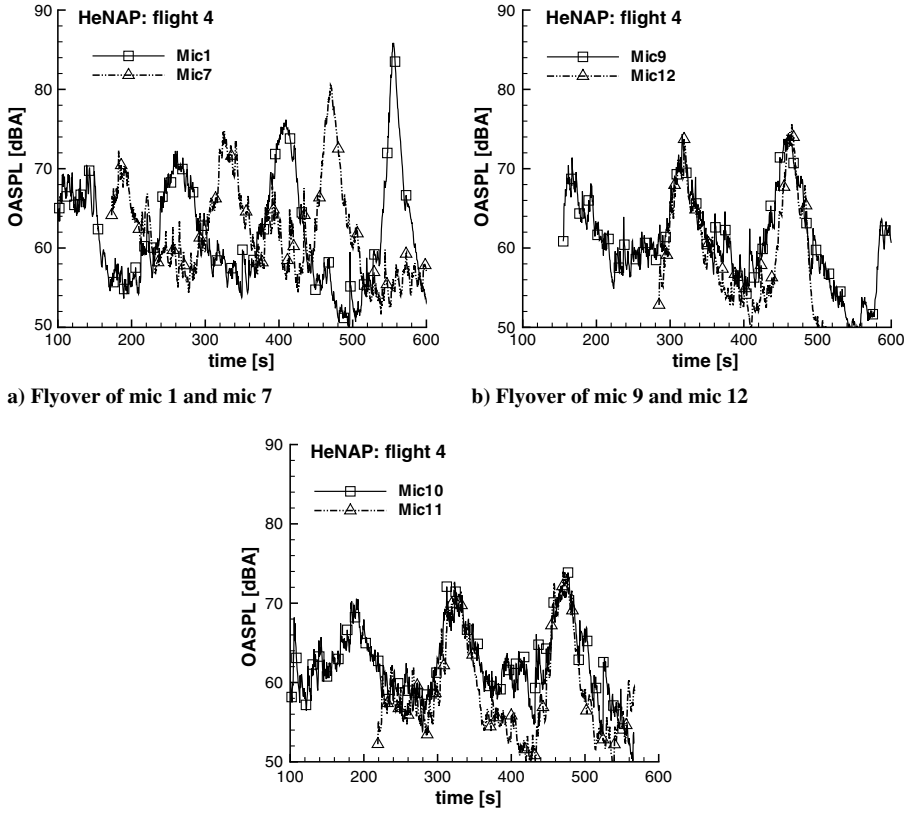

a) Flyover of mic 1 and mic 7

b) Flyover of mic 9 and mic 12

c) Flyover of mic 10 and mic 11

Fig. 11 Flight 4 (HENAP): measured SPL_A time history at observers along the helical flight segment.

have to be neglected. The software was not developed to precisely predict absolute noise levels on the ground but to provide trends as early as possible in the preliminary aircraft design phase. Weather effects, e.g., wind, temperature gradients, and topographic effects, are not accounted for. Unless otherwise indicated, the following setting was applied for the noise prediction with PANAM: ground microphones, no shielding effects, and ground reflection with $\sigma = 100,000\ (\mathrm{kN \cdot s})/\mathrm{m}^4$. Discrepancies between measurement and prediction are expected to increase with large distances between observer and source due to the implemented approximations for atmospheric sound propagation effects [11]. In conclusion, only noise level differences between the tested procedures should be considered for the comparison of experiment and prediction.

Figure 12 depicts predicted maximum SPL_A footprints for HENAP, steep, and standard approach. The noise was predicted based on recorded data during the flight test. Maximum SPL_A was selected to enable direct correlation of the contour plots and the corresponding level time histories. At a ground distance of 12 km to the runway threshold, computations were started and the reference time was set to zero. The noise computation has been stopped right before the approach was aborted to initiate the go-around. Observer locations are marked on the isocontour plots. The aircraft configuration was held constant during all test flights (constant flap setting with deployed gear), hence, ground noise impact is mainly determined by altitude, speed, and thrust setting. The shape of the noise isocontours can be directly correlated with the recorded flight data. Furthermore, the maximum levels can be identified for each microphone in the corresponding level time history plot.

Increased noise levels early along flight 1 can be correlated to a thrust peak between 50–70 s of flight time depicted in Fig. 8a. Flight data shows continuous and widespread idle operation of the engines along the steep approach. This results in notable necking in contours along these engine idle phases as shown in Fig. 12b. Subsequently, engines are temporarily run up to high thrust levels at 135 s of flight time (see Fig. 8b). As a consequence typical engine noise dominated isocontour shapes can be identified in the maximum SPL_A plot.

Figure 13 shows the predicted vs the measured level time history at locations mic 1, mic 4, and mic 6, located along the common approach path. The trends and level differences are in good agreement between computation and experiment, although major discrepancies are experienced for the steep approach procedure. At locations mic 3 to mic 6 the noise predictions are significantly lower than the experimental data. This is the case for both steep approaches; the second steep approach shows similar behavior. According to the thrust setting along the steep approaches (see Fig. 8b) the engine is running at low RPM. Engine noise seems to be significantly underpredicted for idle operation of the specific engine type (see Fig. 14).

Prediction and experimental data at locations mic 8, mic 9, and mic 12 are depicted in Fig. 15. The agreement of the trends and level differences are satisfying with existing discrepancies due to the aforementioned engine noise underprediction and adverse wind conditions.

Overall, predicted and measured noise level differences between individual test flights are in good agreement. For example, the level differences between a HENAP (flight 4) and a reference approach (flight 1) are presented. For the HENAP the following maximum noise level reduction was confirmed by prediction and experiment: $\approx$10 dBA at location mic 3 and $\approx$8 dBA at locations mic 4, mic 5, and mic 6.

Table 4 Recorded SEL (dBA) along the common approach path and along the spiral

Location	Flight 1	Flight 3	Flight 5
Mic 1	89.7	89.7	89.1
Mic 4	84.4	81.4	79.1
Mic 6	81.0	75.7	76.2
Mic 8	——	——	84.6
Mic 9	——	——	82.1
Mic 12	——	——	81.1

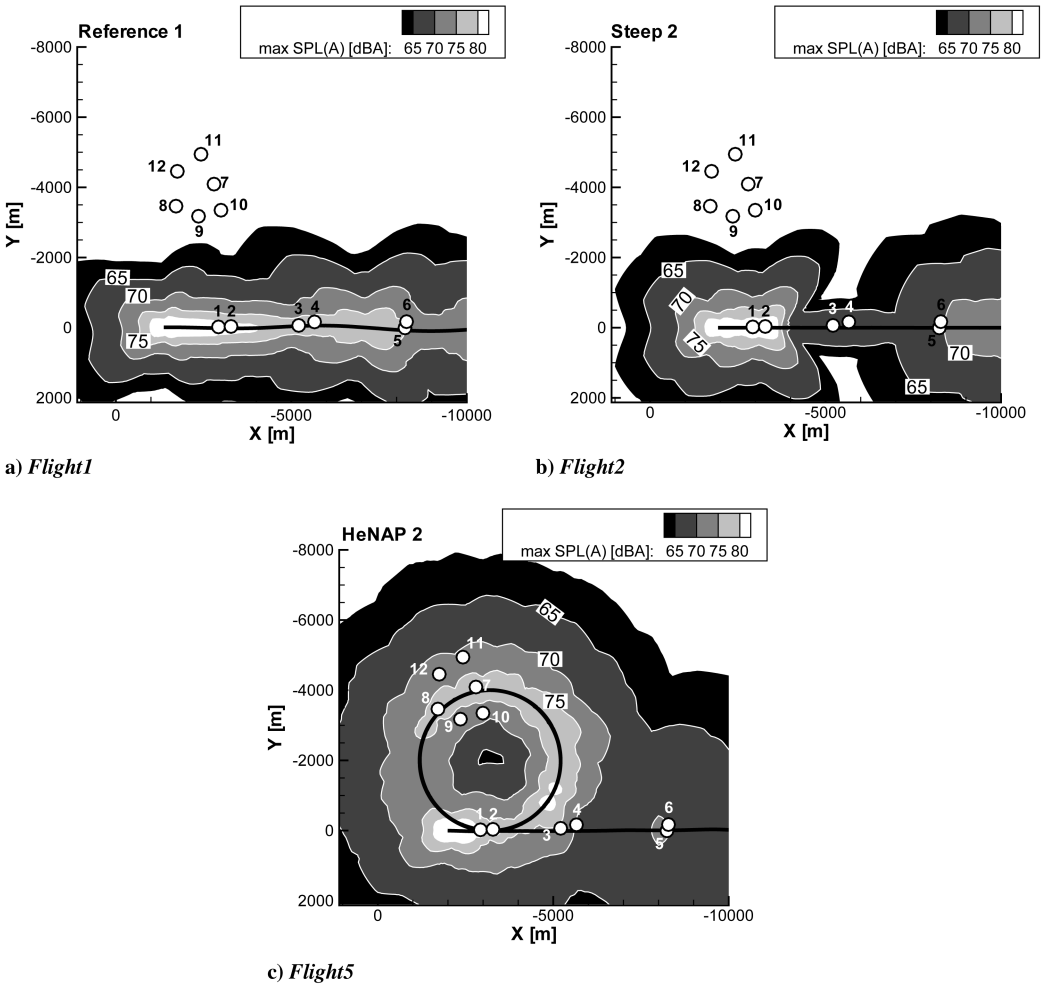

a) *Flight1*

b) *Flight2*

c) *Flight5*

Fig. 12 Flights 1 (reference), 3 (steep), and 5 (HENAP): predicted maximum SPL_A (dBA) isocontours based on recorded flight data during test flights (microphone symbols: circles).

D. Air Traffic Control and Flight Operational Aspects

As already mentioned, the feasibility of integrating the HENAP flight procedure into an existing air traffic scenario should be first prepared and tested at regional airports with a small number of conventional aircraft movements or at times with low air traffic figures (e.g., nighttime where the noise aspect is of paramount importance). The Forschungsflughafen Braunschweig with its location, air traffic, flexibility, and experienced research personnel offers splendid conditions for the initial evaluation of such new operational flight profiles. After the promising results in terms of sound pressure levels dislocation to ideally unpopulated areas for that kind of procedure as described in the sections before, this chapter leaves the perspective of the single event environmental assessment and addresses first subjective comments of an operational implementation of this specific noise reduction approach procedure into a complete air traffic system with multiple flights.

For this reason, the complete flight-test campaign has been attended in the background by research staff from DFS directly from the tower building and the procedures have been kindly reviewed by the two tower controllers on duty (one tower runway and ground controller at one communication frequency, and one tower controller assistant for planning and coordinating issues; note that the tower EDVE is not operated by DFS). Their subjective statements with regard to workload and situational awareness considering the various approaches are summarized next. A radar display based on the system PHOENIX was available for both controllers for the presentation of airborne aircraft positions around EDVE (range normally until flights reach FL150); a further monitor for the specific illustration of surface movements was not at hand. Meteorological parameters, i.e., wind speed and direction, ambient pressure, temperature, and humidity were logged continuously from Forschungsflughafen Braunschweig around the airport ground during the seven approaches and delivered afterwards to the partners for further processing. There was visual contact between the control tower and the flying testbed ATTAS, which flew under instrumented flight rules, throughout all helical segments (visual meteorological conditions). Before commencing each individual approach procedure the corresponding tower controller issued a low approach clearance to the pilots for RWY 26 in coordination with the responsible area control center located in Bremen. Only for the last flight (flight 7, reference approach procedure) there was need for an ILS landing clearance on RWY 26, given 10 n miles before touchdown.

With regard to separation, the vertical separation between two aircraft has to be at least 1000 ft. As the helix initial altitude h_{init} is set at 7500 ft and h_{end} at 550 ft, the aircraft descends about 2300 ft in every spiral (altogether three turns). The length of a completed spiral segment is about 7 n miles. Considering the relative constant flight speed of about 160 kt during the HENAP segments (Fig. 8c) results in a flight time of 150 s for one spiral element.

Horizontal separation minima [12] according to ICAO wake turbulence categories must be applied when both aircraft are landing at the same runway (in our case RWY 26). Radar separation minima between two aircraft are usually 3 n miles below FL 195 (system PHOENIX).

However, as long as wake turbulence behavior within the helical segments has not been further detailed, only one aircraft at a time should be allowed to enter and follow the HENAP in its current design ($n_{\text{turn}} = 3$); which is a very conservative approach considering the before mentioned separation values (ATTAS VFW 614: wake turbulence classification medium).

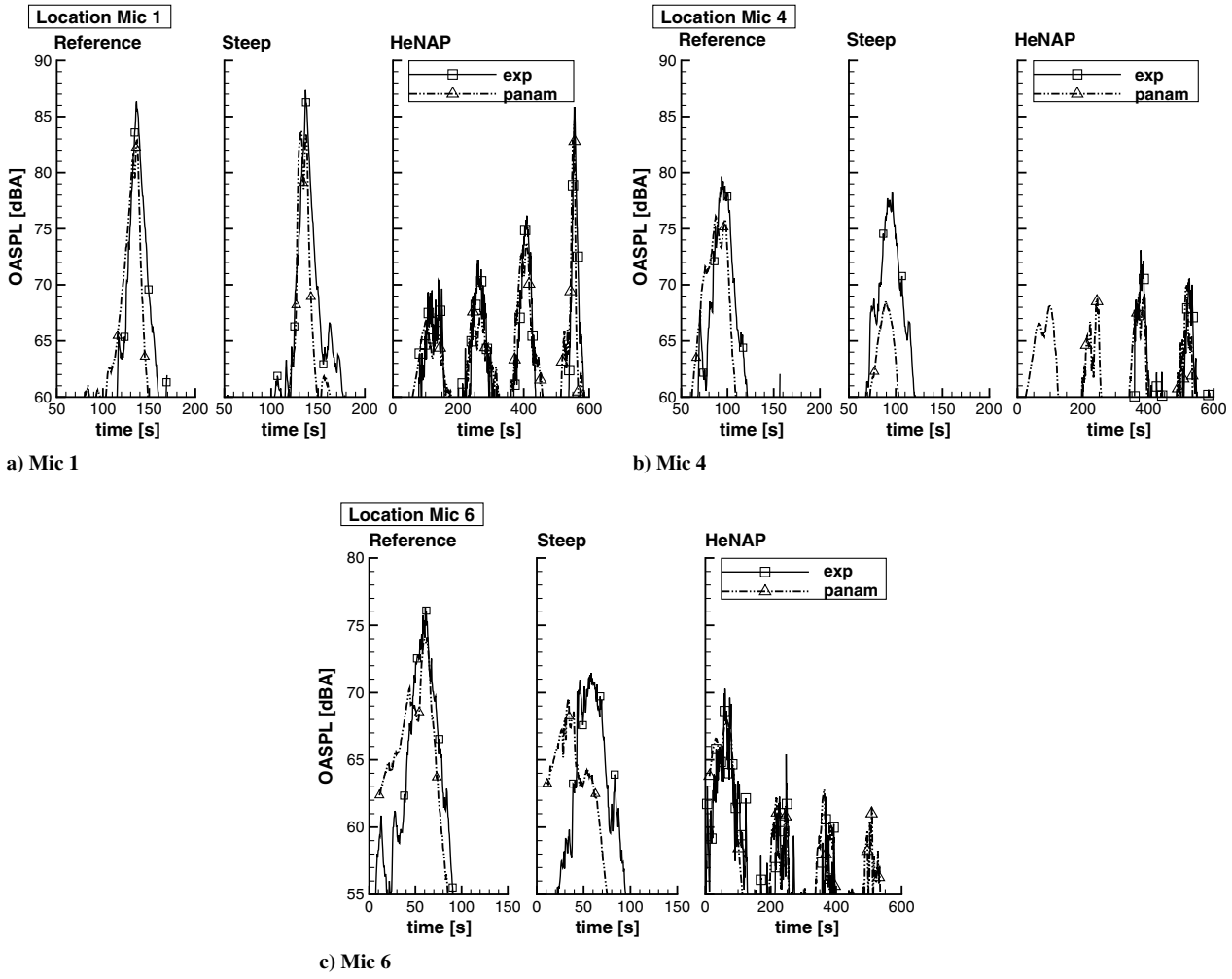

Fig. 13 Flights 1 (reference), 3 (steep), and 4 (HENAP): SPL_A prediction vs experimental data for observer locations along common approach path; mic 1, mic 4, and mic 6.

In dedicated interviews, the tower controllers have been asked to give statements after each approach procedure. Whereas they reported no specific handling and controlling challenges for reference and steep approach procedures, the defined HENAP raised safety and efficiency questions in terms of missed approaches and blocking northbound departures and northern aerodrome traffic circuit for a long time. Therefore a negative influence on the throughput of an airport is estimated; however this task was not in the focus of this study and further analysis is thus necessary. In addition, subjective work load of the involved air traffic controllers increases as they have to watch carefully the altitude information of the ATTAS aircraft on a primarily two-dimensional display and be aware of the number of spiraling segments during HENAP. Summarizing the comments, this kind of noise abatement procedure is not applicable during daytime with current operational state of technology at bigger airports and under adverse weather conditions.

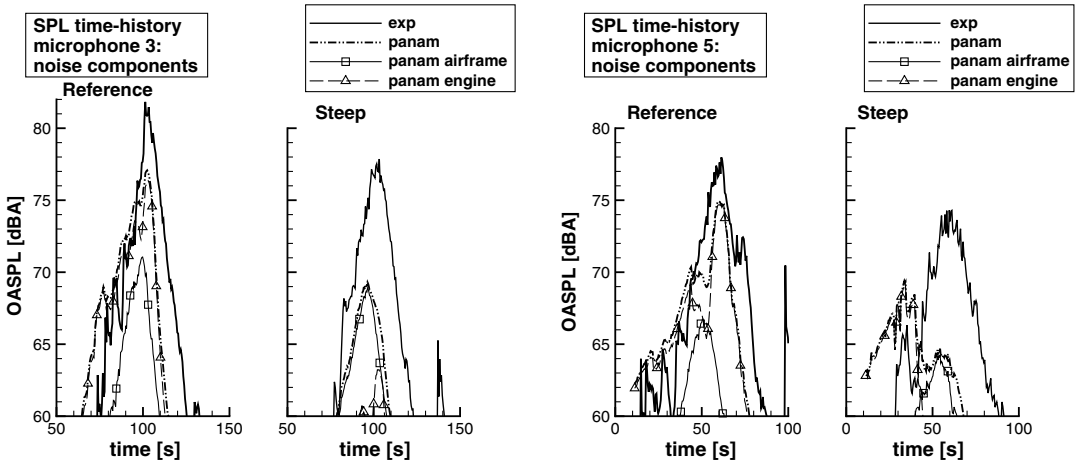

Fig. 14 Flights 1 (reference) and 3 (steep): predicted noise components vs experimental data (SPL_A).

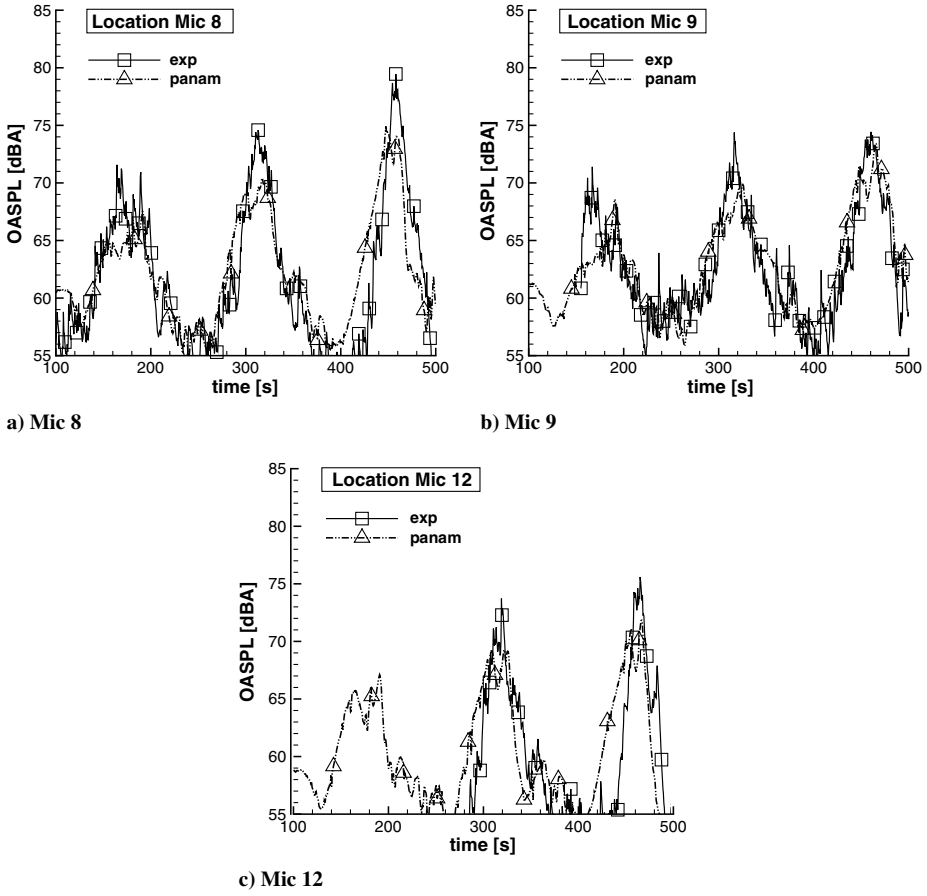

Fig. 15 Flight 4 (HENAP): SPL_A prediction vs experimental data for observer locations along helical flight segments; mic 8, mic 9, and mic 12.

These aspects have to be addressed and clarified in advance before transferring helical noise abatement flight tests to other airports which are confronted with more flight movements.

VI. Conclusions

HENAP is currently under investigation for overall aircraft ground noise reduction. Initial computational studies indicate significant noise reduction potential for this procedure. High ground noise levels can be dislocated from the common ILS approach path and concentrated to the area along the helical flight segments. But at the same time, ground noise levels along the entire preceding flight path are significantly reduced.

Fuel demand, required flight time, and engine emissions along a helical approach are increased if compared with ideal and short direct ILS approaches. The situation could be more advantageous for the HENAP if compared with approaches from any other heading than the runway heading. In this case, the aircraft will be vectored to the vicinity of the airport followed by a complex approach pattern, composed of downwind leg, base leg, and a final approach leg. Ideally, the final path for the standard approach may be even longer implying that more fuel and flight time would be required. Obviously, a case by case evaluation of the specific scenario becomes inevitable.

A systematic operational and economical evaluation has to be performed in the future as this was not possible under the given circumstances. The presented study did not investigate configurational changes along the flight procedures nor evaluate modifications to the geometry of the spiral, e.g., varying radii with steeper spiraling segments. Therefore, it can be expected that the full potential of spiraling approach procedures toward noise reduction with feasible or even beneficial economical implications is yet to be explored.

In parallel to the computational activities, a DLR flight test was prepared to test a newly developed autopilot with improved weather capabilities. The flight-test maneuvers were conducted in the form of landing approaches to investigate both the new autopilot and the HENAP at the same time. For a comparative analysis of the HENAP, a steep approach and a standard ILS approach were included in the test program. The flight tests could be combined with a dedicated ground noise measurement campaign. Ground noise levels have been recorded at selected observer locations along the flight ground track. Measurements confirmed the anticipated noise dislocation effects along the spiraling approach. Compared with the reference approach, maximum SPL_A reduction of approximately 8 dBA was measured at locations mic 5 and mic 6 for the HENAP. Observers located in close vicinity of the helix but not directly along the common approach path are subject to increased community noise pollution due to HENAP operation (SPL_A and SEL). Obviously, these observers experience multiple direct flyover events per each HENAP approach, whereas steep and reference approach are aligned with the common approach path hence do not require any aircraft movement in that area. The test flights have been simulated and noise levels were predicted according to recorded flight data. The predicted and measured noise level differences between individual test flights are in good agreement with the experimental data. Finally, it can be concluded that the applied noise prediction methods are capable of predicting the noise distribution along helical flight procedures. The requirements for a feasible comparative noise evaluation are fulfilled with the existing methods. Technical feasibility of the radical approach procedure has been demonstrated by computational means and by dedicated flight tests.

The tower controllers reported no specific handling and controlling challenges for reference and steep approach procedures but the HENAP raised safety and efficiency questions. Helical approaches increased the subjective work load of the tower controllers. A clear distinction between these first impressions and trends and a later evaluation phase with a detailed operational concept has to be made when interpreting the results of the paper. It

can be summarized that this kind of procedure is not applicable during daytime with current state of technology or under adverse weather conditions. Helical approaches become more feasible for implementation at small, low-frequented regional airports or during night hours to avoid possible noise related curfews. Significant economical benefit due to extended operating hours could be achieved [13].

Acknowledgments

The authors would like to express their gratitude toward the DLR, German Aerospace Center (hereinafter referred to as DLR) ATTAS flight crew, especially M. Press and D. Leißling, for their excellent job in preparing and operating the simulation and the flight test. The authors would like to thank R. Henke (RWTH Aachen University), H. Geyr von Schweppenburg (DLR), and J. Bals (DLR) for their support toward an add-on ground noise measurement campaign. Furthermore, the authors thank R. Henke for supporting the no-budget activities with the necessary acoustical equipment and additional manpower. The permission of local landlords around EDVE to place microphones on their property is greatly appreciated. The authors thank all involved volunteers of DLR and RWTH Aachen University for participating in this extracurricular activity. The authors greatly appreciate the advice and support of C. Hange, NASA Ames Research Center, concerning spiraling approach procedures and their possible application. Finally, the authors thank the peer reviewers for their recommendations and valuable input.

References

[1] Bertsch, L., Looye, G., Lummer, M., and Otten, T., "Integration and Application of a Tool Chain for Environmental Analysis of Aircraft Flight Trajectories," AIAA Paper 2009-954, Sept. 2009.

[2] Hange, C., and Eckenrod, D., "Assessment of a C-17 Flight Test of an ESTOL Transport Landing Approach for Operational Viability, Pilot Perceptions and Workload, and Passenger Ride Acceptance," AIAA Paper 2007-1398, 2007.

[3] Young, J. R., and Hall, D. W., "Executive Summary of Cal Poly/NASA Extreme Short Takeoff and Landing (ESTOL) Work," AeroTech Congress and Exhibition 2005, SAE Paper 2005-01-3177, 2005.

[4] Looye, G., "Flight Testing of Autopilot Control Laws: Fly the Helix!," German Aerospace Congress 2009, DLRK Paper 2009-121375, 2009.

[5] Lummer, M., "Maggi-–Rubinowicz Diffraction Correction for Ray-Tracing Calculations of Engine Noise Shielding," AIAA Paper 2008-3050, 2008.

[6] Bertsch, L., Dobrzynski, W., and Guérin, S., "Tool Development for Low-Noise Aircraft Design," *Journal of Aircraft*, Vol. 47, No. 2, March–April 2010, pp. 694–699. doi:10.2514/1.43188

[7] "FUTSU Night North Arrival," Civil Aviation Bureau Japan Rept. RJTT-AD2-24.36 [online report], http://www.opennav.com/airport/RJTT [retrieved 18 Nov. 2010].

[8] "International Standards and Recommended Practices, Environmental Protection, Annex 16 to the Convention on International Civil Aviation," *Aircraft Noise*, 5th ed., Vol. 1, Aviatech, Montreal, July 2008.

[9] Dobrzynski, W., "Interferenzwirkungen durch Bodenreflexion bei Fluglaermmessungen an Propellerflugzeugen," DFVLR-Forschungsbericht Rept. FB 81-28, 1981.

[10] Pott-Pollenske, M., Dobrzynski, W., Buchholz, H., Guérin, S., Saueressig, G., and Finke, U., "Airframe Noise Characteristics from Flyover Measurements and Predictions," AIAA Paper 2006-2567, 2006.

[11] "American National Standard Method for the Calculation of the Absorption of Sound by the Atmosphere," American National Standards Institute Rept. S1.26-1978, 1978.

[12] "DFS: Manual of Operations for Air Traffic Control Services," Betriebsanweisung Flugverkehrskontrolle, DFS Deutsche Flugsicherung GmbH, Langen, Germany, 22 Nov. 2007, p. 32 ff.

[13] Wan Mohamed, W. M., Curran, R., van der Zwan, F., and Roling, P., "Modeling the Effect of Night Time Penalties on Commercial and Business Flights for Regional Airport Noise and Economics: Rotterdam Airport Case Study," AIAA Paper 2009-7086, 2009.